

Studies on the Adsorption Behavior of La^{3+} , Ce^{3+} , Nd^{3+} and Sm^{3+} on Synthesized Poly-O-Toluidine Zr (IV) Tungstophosphate Composite

E.S.Zakaria¹, I. M.Ali¹, M.Khalil¹, T.Y.Mohamed² and A.El-Tantawy¹

¹Atomic Energy Authority, Hot Laboratories Center, P. O. Box 13759, Egypt

²Chemistry Dept., Faculty of Science, Benha Univ., Benha, Egypt

E-Mail: dr_Talaat2003@yahoo.com

Abstract

Various samples of poly-*o*-toluidine Zr(IV) tungstophosphate (POTZr(IV)WP) composite exchanger were synthesized with different molar ratios. Determination of the sample which showed maximum Na^+ exchange capacity was selected for further studies. The ion-exchange capacity, chemical stability, effect of resin dosage, pH titration were carried out to understand the ion-exchange capabilities. The physico-chemical properties of materials were determined using CHN, elemental analysis, FTIR, TGA–DTA, XRD, XRF and SEM studies. The material showed good ion-exchange behavior for La^{3+} , Ce^{3+} , Nd^{3+} and Sm^{3+} ions. Sorption isotherm studies were performed at different reaction temperatures and analyzed by Langmuir, Freundlich, Dubinin-Raduchkivich and Temkin isotherm models and found to follow Langmuir model. Thermodynamic parameters such as ΔG° , ΔH° and ΔS° were determined and found to be endothermic and spontaneous in nature. This study may have great potential in developing high performance composite for lanthanide separation.

Keywords: ion exchanger; characterization; sorption; isotherm; *o*-toluidine.

1. Introduction

In the last decades, the demand for rare earth elements (REE) was increased due to development of many advanced technologies. So REE have received great attention due to their importance in different applications like electronics, catalysts, used in clean energy technologies of the future such as wind turbines, electric vehicles and phosphors. REE are produced during the uranium fission and present in the radioactive waste [1]. REE-rich sources, have rare earth oxides (REO), such as carbonate-based bastnasite and phosphate based monazite. Lanthanide group elements are chemically similar, so their separations are difficult. Lanthanide separation and purification are important for controlling of radioactive wastes, renewable energy technologies of the future, mining industries as well as environmental remediation and pollution control. As result of being fission product REE can be used as non-active simulators to investigate the expected behavior of the long-lived, radiotoxic minor actinides [1].

Different technologies are applied for the purpose of separation and purification such as chemical precipitation, coagulation, sedimentation, flotation, filtration, membrane processes, electrochemical techniques, ion exchange, biological processes and chemical reactions. One of the most promising technologies widely applied for metal ions retention is ion exchange. This technique has many advantages such as the simplicity of equipment, operation and regeneration [2]. In the early days, organic resins are introduced for remediation of waste waters that may contain toxic, radioactive or precise metal ions. These organic resins are preferably used in certain process such as water treatment due to their high ion exchange capacity, good mechanical properties but they have limitations such as poor thermal, chemical and radioactive stability, they able to swell and they have no selective behavior for specific metal ions[3].

Due to the limitations of organic resins, researchers developed inorganic ion exchangers that have good chemical, thermal and radiation stability, selectivity for specific metal ions but they have limitations low capacity compared to organic resins and irreproducibility [4]. Most of the inorganic ion exchangers [5,6,7] such as lithium titanate, tin silicate, tin and titanium-ferrocyanides, etc., exhibit very low ion exchange efficiency in the high acidic media.

Many researchers take great attention to create a new class of hybrid organic–inorganic ion exchangers to combine the main. Advantages of each constituent [8]. These hybrid ion–exchangers consisting of inorganic ion exchangers and organic binding matrices. Composite ion exchangers are favorably used as they have many advantages such as improved mechanical properties due to binding of organic polymer, its granulometric properties that makes them more suitable for the application in column operations. Chemical inertness, high thermal and radiation stability, reproducibility and high selectivity. so they able to make direct conversion to stable crystalline phases from which radionuclides cannot be leached. This makes such materials suitable for direct disposition for the disposal of long-lived heat-producing radionuclides. In this study various samples of Poly-*o*-toluidine Zirconium tungstophosphate (POTZr(IV)WP) with different molar ratios were prepared to obtain the most effective sample can be used for retention of important metal ions as La^{3+} , Ce^{3+} , Sm^{3+} and Nd^{3+} from aqueous solution. POTZr(IV)WP composite material was characterized by FTIR, XRD, TG-DTA, XRF, SEM and CHN elemental analysis, chemical stability and pH titration curve. Effect of resin dosage experiment was studied to determine the optimum V/m used in batch experiments. Sorption isotherm

studies were conducted in order to investigate the sorption mechanism controlled the sorption process of La³⁺, Ce³⁺, Sm³⁺ and Nd³⁺ onto POTZr(IV)WP.

2. Materials and methods

2.1 Chemicals and reagents

The main reagents used for the synthesis were zirconium oxychloride (ZrOCl₂·8H₂O), N-Cetyl-N,N,N-trimethyl ammonium bromide, CTAB (C₁₉H₄₂BrN), sodium dodecyl sulphate, SDS (CH₃(CH₂)₁₁OSO₃Na), was obtained from ELNASR PHARMACEUTICAL CHEMICALS CO. EGYPT. Sodium dioctylsulphosuccinate, SDSC (C₂₀H₃₇NaO₇S), was obtained from KAMSONS CHEMICALS PVT.LTD, INDIA. Potassium persulphate (K₂S₂O₈) was obtained from LOBA CHMIE, INDIA. Sodium tungstate (Na₂WO₄·2H₂O), ortho-toluidine (C₁₄H₁₈Cl₂N₂), nitric acid, acetic acid, orthophosphoric acid and hydrochloric acid were purchased from Adwic, Egypt. Neodymium(III) nitrate hexahydrate was purchased from FLUKA. Samarium(III) chloride hexahydrate was purchased from STREM CHEMICALS, UNITED STATES. Cerium(III) nitrate hexahydrate was purchased from MERCH, GERMANY. Lanthanum (III) chloride hexahydrate was purchased from WINLAB. All other reagents and chemicals were of analytical grade purity.

2.2 Preparation of the reagent solutions

Various concentrations of zirconium oxychloride, sodium tungstate and Ortho-phosphoric acid solutions were prepared in bidistilled water while the solutions of o-toluidine (0.28 M) and potassium persulphate (0.1 M) were prepared in 1 M HCl solution.

2.3 Synthesis of adsorbent materials

Various adsorbents were synthesized as poly-o-toluidine, zirconium tungstate, zirconium tungstophosphate and poly-o-toluidine zirconium tungstophosphate with different methods.

2.3.1 Synthesis of poly-o-toluidine

A polymer of o-toluidine gels were prepared by mixing an equal volume ratio of the solution of 0.1 M potassium persulfate and 0.14 M o-toluidine. The solution of potassium persulfate was added drop by drop in the flask containing o-toluidine with continuous stirring at the room temperature. Potassium persulfate acted as an oxidizing agent resulting in the formation of polymer gel which was kept for 1 h at room temperature [9].

2.3.2 Synthesis of zirconium tungstate (Zr(IV)W) with hydrothermal method

Hydrothermal technique was used for preparation of zirconium tungstate 200 ml (0.1 M) sodium tungstate solution was added drop wise to 200 ml

(0.1M) zirconium oxychloride solution and 0.2 g CTAB with continuous stirring by magnetic stirrer at room temperature (25 ± 1 oC). The pH of the mixture was adjusted at 1.5 by adding an aqueous solution of ammonia or nitric acid with constant stirring. Then, the white colored gel was transferred into a Teflon-lined stainless steel autoclave (400 ml) to carry out hydrothermal reactions at 150 oC for 24 h. After the autoclave was allowed to cool at the room temperature naturally, the supernatant liquid was decanted and the gel was rewashed with bidistilled water in order to remove fine adherent particles then filtered by using a centrifugation (about 4000 rpm). The excess acid was removed by washing with bidistilled water and the material was dried in an air oven at 60 ± 1 oC. The dried product was immersed in bidistilled water to obtain small granules. The material was converted to H⁺ - form by treating with 0.1 M HNO₃ for 24 h with occasional shaking intermittently replacing the supernatant liquid with fresh acid. The excess acid was removed after several washings with bidistilled water and then dried at 60 ± 1 oC. Several particles size of material was obtained by sieving and kept for further usage in the batch experiments [10].

2.3.3 Synthesis of zirconium tungstate (Zr(IV)W) with sol gel method

Various samples of inorganic precipitate of Zr(IV)tungstate was prepared at room temperature based on using different surfactants (CTAB, SDS and SDSC). The solution of 0.1M sodium tungstate to a mixture aqueous solution of 0.1 M zirconium oxychloride and (0.1g of CTAB, 0.5g of SDS and 1ml of SDSC) with continuous stirring by magnetic stirrer at (25 ± 1°C). Then the pH of the obtained mixture was adjusted at 1.5 by adding an aqueous solution of ammonia or nitric acid with constant stirring. Zirconium tungstate was obtained as white colored gel.

2.3.4 Synthesis of zirconium tungstophosphate (Zr(IV)WP)

Zirconium tungstophosphate inorganic ion exchanger was prepared by adding a mixture aqueous solution of 0.1 M sodium tungstate and 4 M H₃PO₄ gradually to a mixture aqueous solution of 0.1 M zirconium oxychloride and 0.1 g of cetyl trimethyl ammonium bromide with continuous stirring by magnetic stirrer at (25 ± 1 oC). The pH of the mixture was adjusted at 1.5 by adding an aqueous solution of ammonia or nitric acid with constant stirring. Then white colored gel was obtained as zirconium tungstophosphate [11].

2.3.5 Synthesis of poly-o-toluidine zirconiumtungstate (POTZr(IV)W)

Poly-o-toluidine Zr (IV) tungstatecation exchanger was prepared by sol-gel method through different mixing ways.

2.3.5.1 Synthesis of POTZr (IV) W by normal method

In this method the organic polymer of o-toluidine was added to the inorganic precipitate of Zr(IV)tungstate with constant stirring. The resultant mixture turned slowly into brownish green colored slurries. The obtained solution pH was adjusted to 1.5 by ammonia solution or nitric acid. The obtained slurries were kept for 24 h at room temperature $25 \pm 1^\circ\text{C}$ for digestion. Then as mentioned below [9].

2.3.5.2 Synthesis of POTZr(IV)W by chelation method

In this method the hybrid material was prepared by adding solution of 200ml (0.1M) sodium tungstate to the mixture solution of 100ml (0.1M) zirconium oxychloride, 0.1g CTAB and 50ml (0.05M) o-toluidine then adding 50ml (0.1M) $\text{K}_2\text{S}_2\text{O}_8$. The obtained mixture solution pH value adjusted to 1.5 by ammonia solution or nitric acid. The obtained slurries were kept for 24 h at room temperature $25 \pm 1^\circ\text{C}$ for digestion. Then as mentioned below.

2.3.5.3 Synthesis of POTZr(IV)W by insitue method

In this method the composite material was prepared by adding the mixture solution of 200ml (0.1M) sodium tungstate and 50ml (0.1M) $\text{K}_2\text{S}_2\text{O}_8$ drop wisely to mixture solution of 50ml (0.05M) o-toluidine and 100ml (0.1M) zirconium oxychloride with 0.1g CTAB. The resultant mixture turned slowly into brownish green colored slurries. The obtained solution pH was adjusted to 1.5 by ammonia solution or nitric acid. The obtained slurries were kept for 24 h at room temperature $25 \pm 1^\circ\text{C}$ for digestion. The supernatant liquid was decanted and the gel was rewashed with bidistilled water in order to remove fine adherent particles then filtered by using a centrifugation (about 4000rpm). The excess acid was removed by washing with bidistilled water and the material was dried in an air oven at $60 \pm 1^\circ\text{C}$. The dried product was immersed in bidistilled water to obtain small granules. The material was converted to H^+ -form by treating with 0.1 M HNO_3 for 24 h with occasional shaking intermittently replacing the supernatant liquid with fresh acid. The excess acid was removed after several washings with bidistilled water and then dried at $60 \pm 1^\circ\text{C}$. Several particles size of material was obtained by sieving and kept for further usage in the batch experiments. In this way a number of samples of poly-o-toluidine-Zr(IV)tungstate were synthesized under variable conditions. Then sodium ion exchange capacities were 0.16, 0.15 and 0.24 for the normal, chelation and insitue methods respectively. On the basis of the highest ion exchange capacity (0.24meq g^{-1}), sample prepared by insitue method was selected for further preparation studies as in Table (1).

2.3.6 Synthesis of poly-o-toluidine Zr (IV) tungstophosphate (POTZr(IV)WP)

POTZr(IV)WP was synthesized with different molar ratios to obtain the best sample. Where 0.05, 0.1, 0.15 and 0.28 M o- toluidine was added to mixture solution of 0.1 M $\text{ZrOCl}_2 \cdot 8\text{H}_2\text{O}$ and 0.1M $\text{Na}_2\text{WO}_4 \cdot 2\text{H}_2\text{O}$ then the obtained slurries were washed with bidistilled water and dried at 60°C . Then immersed in HNO_3 , washed again several times, dried and kept in a desiccator for further studies.

poly-o-toluidine Zr(IV)tungstophosphate cation exchanger was prepared by sol-gel insitue method as the mixture solution of 200 ml (0.1 M) sodium tungstate, 50 ml (0.1 M) $\text{K}_2\text{S}_2\text{O}_8$ and 50 ml (4 M) H_3PO_4 drop wisely to mixture solution of 50ml (0.05 M) o-toluidine and 100 ml (0.1 M) zirconium oxychloride with 0.1 g CTAB with constant stirring using the best conditions for the preparation of Zr(IV)tungstate in the above section. The resultant mixture turned slowly into brownish green colored slurries. The resultant slurries were kept for 24 h at room temperature $25 \pm 1^\circ\text{C}$ for digestion. The supernatant liquid was decanted and the gel was rewashed with bidistilled water in order to remove fine adherent particles then filtered by using a centrifugation (about 4000 rpm). The excess acid was removed by washing with bidistilled water and the material was dried in an air oven at $60 \pm 1^\circ\text{C}$. The dried product was immersed in bidistilled water to obtain small granules. The material was converted to H^+ -form by treating with 0.1 M HNO_3 for 24 h with occasional shaking intermittently replacing the supernatant liquid with fresh acid. The excess acid was removed after several washings with bidistilled water and then dried at $60 \pm 1^\circ\text{C}$. Several particles size of material was obtained by sieving and kept for further usage in the batch experiments [9]. In this way a number of samples of poly-o-toluidine-Zr(IV)tungstophosphate were synthesized under variable conditions Table (1). On the basis of the highest ion exchange capacity (1.8meq g^{-1}) together with physical stability and appearance of beads, sample S-17 was selected for detailed studies.

2.4 Chemical stability

In order to measure the stability of composite against various media. The chemical stability of POTZr(IV)WP in various media – acids (HCl and HNO_3), base (NaOH), organic solvent (acetic acid) and also with double distilled water (DMW) was studied by batch experiments as follows: 50 mg portions of POTZr(IV)WP were contacted for 24 h at room temperature with 50 ml of a particular medium with intermittently shaking. After contact, the ion exchanger were separated then dried at 70°C and the weight losses (%) were calculated.

2.5 Sodium ion exchange capacity (IEC)

The ion exchange capacities of different prepared ion exchangers were determined by acid–base titration. The weighted sample of the ion exchanger in its H⁺ form were soaked in 50 mL of 1 M NaCl solution for at least 12 h with shaking at ambient temperature to exchange protons with sodium ions. The ion exchanged solution was titrated to the phenolphthalein end point (2 drops of ph.ph indicator, 1% ph.ph in ethanol) with a NaOH solution of 0.1M concentration. The ion exchange capacity (IEC) was calculated using the following equation:

$$IEC(\text{meq./g}) = V_{\text{NaOH}} \frac{C_{\text{NaOH}}}{W_d} \quad (1)$$

where V_{NaOH} , C_{NaOH} and W_d are the volume of NaOH consumed in titration, the concentration of NaOH solution, and the weight of the dry sample, respectively.

2.6 pH titration curve

2.6.1 pH titration

In order to determine the functionality behavior of POTZr(IV)WP. The pH titration studies were performed by Topp and Pepper method [12,13]. Each 0.05 g of POTZr(IV)WP composite cation exchanger in H⁺ form were placed in each of the several glass bottles containing equimolar solution of alkali metal chlorides and their corresponding hydroxide in different volume ratios such as NaCl–NaOH, LiCl–LiOH, KCl–KOH systems. The final volume being kept at 10 ml to maintain the ionic strength constant with intermittent shaking. The pH of the solution was recorded after every 24 h till the equilibrium was attained. The pH of the solution was determined after attaining the equilibrium (which needed about 7 days) and the pH was plotted against the mill equivalents of (OH⁻) ions that were added.

2.7 Elemental composition of POTZr (IV)WP

To determine the elemental composition of POTZr(IV)WP, the material was analyzed for Zr and W by X-ray fluorescence. Where P is determined by ICP by dissolution of the material in acid such as H₂SO₄ and Carbon, hydrogen and nitrogen contents of the material were determined by elemental analysis

2.8 Effect of resin dosage

In order to obtain the optimum batch factor (V/m) used for performing the experiments, where different adsorbent masses (0.025, 0.033, 0.05, 0.1, 0.2 and 0.4g) of POTZr(IV)WP were conducted with 10 ml of 50 mgL⁻¹ samarium(III)chloride solution in several stoppered glass bottles and kept in the thermostatic shaker water bath at room temperature for sufficient time to obtain the equilibrium. The supernatant solutions were analyzed using UV-Visible Spectrophotometer and the percent uptake was calculated as the following:

$$\%Uptake = \frac{C_0 - C_e}{C_0} \times 100 \quad (2)$$

Where C_0 and C_e are the initial and equilibrium concentrations of metal ion in mgL⁻¹

2.9 Instruments and characterization of the prepared materials

Measurements of powder X-ray diffraction patterns were carried out using Shimadzu X-ray diffractometer, Model XD 490, Shimadzu, Japan, with a nickel filter and Cu- K_α radiation tube. Samples were very lightly ground and mounted on a flat sample plate at room temperature. The average crystal size of the powder is calculated from diffraction peak full width at half maximum (FWHM), using the Scherrer equation. Scanning electron microscopy (SEM) was performed using a high-resolution scanning electron microscope XL30 SFEQ, Phillips, the Netherlands. The Fourier transform infrared spectra were recorded using an FTIR spectrometer, using Nicolet is10 spectrometer from Meslo, USA, product from USA in the range of 4000–400 cm⁻¹ with 32 scans at a resolution of 2 cm⁻¹ using KBr disc technique. The thermal stability of prepared compounds was ascertained by thermogravimetric analysis (TGA) and differential thermal analysis (DTA). Shimadzu DTA–TGA system of type DTA-TGA-60, Japan with platinum crucible and alumina powder reference was used for the measurements of the phase changes and weight losses of the sample, respectively. Samples were heated up to a temperature of 1000 °C in the presence of nitrogen atmosphere to avoid thermal oxidation of the powder sample with a heating rate of 20 °C min⁻¹. The metal ions concentration were measured using UV-Visible spectrophotometer, Shimadzu, Japan, and an inductively coupled plasma atomic emission spectroscopy, ICPs-7510, Shimadzu, Japan. All the pH values of different solutions were measured using pH a glass electrode, AD/030, Romania with microprocessor and have accuracy of ±0.02 units. The pH meter scale was calibrated using two standard buffer solutions within the pH range of the measured solution before each experiment. The deviation in the readings was in the range of ±0.01 at the laboratory temperature 25 ±1 °C. A thermo stated shaker, Clifton, England was used for ion exchange equilibrium experiments. All samples and chemicals used in this work were weighted using an analytical balance of ae ADAM, pw124, Germany, having maximum sensitivity of 120g and accuracy ±0.0001g.

2.10 Sorption isotherm studies

Sorption process of the studied metal ions (La³⁺, Ce³⁺, Nd³⁺ and Sm³⁺) onto POTZr(IV)WP was carried out to investigate the adsorption mechanism and other surface properties as adsorbent affinity. Sorption experiments were performed by batch method. where 50 mg of the adsorbent material

conducted with 5ml metal ion solutions of [La, Ce and Sm chlorides] and Nd nitrate with concentration ranges from (100-1000 mgL⁻¹) where pH of the prepared metal ion solutions were kept constant at the optimum neutral pH. The samples established in thermostatic shaker water bath at desired reaction temperatures (25, 45 and 65 ±1°C) until reached the equilibrium time. The supernatant solution was analyzed to determine equilibrium metal ion concentration using UV-Visible spectrophotometer and the adsorption capacity calculated from the following equation:

$$\text{mg g}^{-1} \quad q_e = (c_0 - c_e) \frac{V}{m} \quad (3)$$

Where, q_e is the amount of metal ion sorbed when equilibrium is attained (mg g⁻¹). C_0 and C_e are the initial and equilibrium concentration (mg L⁻¹) of metal ion solution, V is the volume of the solution (L), m is the weight (g) of the adsorbent.

The most common models used for studying sorption isotherm are Langmuir, Freundlich, Dubinin-Radushkivech and Temkin isotherm models. Where Langmuir model assumes that monolayer adsorption which occur at finite number of active sites, which are identical and equivalent (all sites have equal affinity for the adsorbate) with no transmigration of the adsorbate in the plane of the surface. Freundlich isotherm model is the earliest known relationship describing the non-ideal and reversible adsorption, not restricted to the formation of monolayer. This empirical model can be applied to multilayer adsorption, with non-uniform distribution of adsorption heat and affinities over the heterogeneous surface. D-R model was used to distinguish the physical and chemical adsorption of metal ions with its mean free energy, E per molecule of adsorbate (for removing a molecule from its location in the sorption space to the infinity). Temkin model assumes that the heat of adsorption (function of temperature) of all molecules in the layer would decrease linearly with coverage. All molecules adsorbed into the adsorbent have a uniform distribution of binding energies.

3. Result and discussion

3.1 Characterization of materials

3.1.1 IR spectra

The FTIR spectra of poly-*o*-toluidine, zirconium tungstophosphate, poly-*o*-toluidine Zr(IV) tungstophosphate are shown, respectively in Fig (1A,1B,1C) Poly-*o*-toluidine spectrum Fig (1A) include peak at 1559 cm⁻¹ corresponding to C=C stretching vibration. The peak appeared at 1481 cm⁻¹ related to N-H bending vibration band. Peak at 1294 cm⁻¹ due to C-N stretching vibration band. Peak at 1108 cm⁻¹ attributed to C-C stretching vibration. N-H rocking band appeared at 806 cm⁻¹.

Fig (1B) represented IR Spectrum of Zr(IV)WP, the broad band at 3445 cm⁻¹ due to -OH stretching

vibration band of free water molecules. Peak at 1621 cm⁻¹ due to H-OH bending vibration. peak at 1034 cm⁻¹ due to phosphate group. Peak appeared at 800 cm⁻¹ and 600 cm⁻¹ due to metal oxide bonds. IR spectrum of POTZr(IV)WP hybrid material presented in Fig (1C) shows number of peaks related to the function groups present in the material. The material have external water molecules -OH groups [14], metal oxygen bond, phosphate group. The strong and broad peak observed at 3426 cm⁻¹ corresponding to -OH stretching vibration band and these surface -OH groups may act as the sites of exchange [15]. C-H stretching vibration observed at 2921 and 2847 cm⁻¹. The H-O-H bending vibration band observed at 1636 cm⁻¹. Peak at 1559 cm⁻¹ due to C=C stretching vibration band. C- N stretching and N-H bending vibration bands observed at 1380 and 1490 cm⁻¹ respectively. The peak observed at 1052 cm⁻¹ due to Phosphate group. Peaks observed at 814 and 604 cm⁻¹ corresponding to metal oxygen bonds.

3.1.2 Thermal analysis

TG-DTA curve of poly-*o*-toluidine Zr(IV) tungstophosphate are presented in (Fig. 4). At first continuous mass weight loss (about 5.472%) up to 200 °C, which may be due to removal of external water molecule. A steep weight loss observed in the temperature range 200 -700 °C which may be due to decomposition of organic part of the material. above 700 °C very slight (negligible) mass weight loss observed may be due to the formation of metal oxide forms of the material. Where XRD data confirmed the formation of metal oxide as obtained from TGA-DTA curve. The material is stable as the total mass weight loss was 29.357 % up to 1000 °C. Fig (5) shows TGA-DTA curve Zr(IV) tungstophosphate the total weight loss was found 17.9 % up to 800 °C. It was less than POTZr(IV)WP weight loss due to the later contain organic part decomposed at more than 200 °C so the total weight loss of composite material increased.

3.1.3 X-ray diffraction pattern

According to XRD pattern of poly-*o*-toluidine Zr(IV) tungstophosphate shown in Fig.4. It was observed that the material has semi-crystalline nature. The crystallite size, D , was estimated by calculating the broadening of the more intensity diffraction peak (strongest peak) according to the Scherrer equation.

$$D = K\lambda/\beta \cos\theta \quad (4)$$

Where K is the Scherrer constant, which depend upon lattice direction and crystallite morphology (0.9 is used in this study), and β is the FWHM given in radians. $D = 1.081$ nm.

3.1.4 Scanning electron microscope (SEM) studies

In order to know the surface morphology of poly-*o*-toluidine, Zr(IV)WP and POTZr(IV)WP composite

material SEM was used. From Fig (5A,5B,5C) which represent the SEM photographs of poly-o-toluidine, Zr(IV)WP and POTZr(IV)WP composite material, respectively. It clarify that the composite picture was different from poly-o-toluidine and ZWP pictures. The difference in surface morphology may be related to formation of POTZr(IV)WP composite by binding the polymer with Zr(IV)WP. According to Fig (5C) it can be seen that POTZr(IV)WP was spherically shaped.

3.1.5 Chemical stability

The chemical stability of the studied samples in the aggressive media is shown in Fig (2). From this table, it can be seen that POTZr(IV)WP resin have good chemical stabilities in 0.1 to 4 M HCl and 0.1 to 4 M HNO₃ aqueous solutions. The chemical stability of POTZr(IV)WP in HNO₃ was good than in HCl. POTZr(IV)WP has fairly stable in CH₃COOH and NaOH media. The chemical stability may be due to the presence of binding polymer, which can prevent the dissolution of heteropolyacids sols or leaching of any constituent element into the solution [16]. Chemical stability of this resin is much higher than that of the similar materials obtained on the base of POT resins. Thus exchanger is chemically resistant to most of the solvents and can be successfully used with diverse solvents in column operation.

3.1.6 Elemental composition of POTZr(IV)WP

From XRF elemental composition data and CHN elemental analysis the weight composition percent of the material was found to be Zr, 22.13 %; W, 44.603%; P, 7.514%; C, 20.398%; H, 1.956% and N, 3.398% .

The corresponding molar ratio of Zr, W, P, C, HandN Was calculated as 1:1:1:7:8:1 which can suggest the following formula: [(ZrO₂)(WO₃)(PO₄)(-C₇H₆NH-)].nH₂O

The mass weight loss 5.47% which lost at 200 °C represented by TGA curve must be due to the loss of nH₂O from the above structure. Alberti's equation used to calculate the value of n as the following :

$$18n = \frac{X(M+18n)}{100} \quad (5)$$

Where X is the weight loss percent (5.472%) of the exchanger by heating up to 200 °C and (M +18n) is the molecular weight of the material. It was found that n = 1.78 per molecule of the cation exchanger. It was observed that crystalline water molecules can used as active site for exchange process.

3.1.7 PH titration curve

The pH titration curves for POTZr(IV)WP composite cation exchanger was obtained under equilibrium conditions with solutions of NaCl–NaOH, LiCl–LiOH and KCl–KOH systems shows two inflection points which indicate the bifunctional of the cation exchange behavior as in Fig (6) .The nano-composite material appear to be strong cation-

exchanger as indicated by a low pH (~3) of the solutions when no OH⁻ ions were added to the system. With further addition of OH⁻ ions to the metal chloride solution the pH increases rapidly as H⁺ liberated from the material and replaced with alkali ions until the solution was neutralized and acidic groups of hybrid cation-exchanger are completely converted to the alkali form. This means that all H⁺ ions on the hybrid cation-exchanger were exhausted and replaced with alkali ions and the numbers of H⁺ liberated from the material were equivalent to the same amount of alkali interred. It is interesting to note that, H⁺– Na⁺ exchange was faster in comparison to H⁺– Li⁺ and H⁺–K⁺ exchanges as evident from lower pH values in case of NaCl–NaOH system indicating higher release of H⁺ ions [17]. Thus rate of exchange of H⁺ in POTZr(IV)WP composite cation exchanger was found to be in order of Na⁺> Li⁺> K⁺.

3.1.8 Effect of resin dosage

The effect of POTZr(IV)WP dosage on the percent removal of Sm(III) ion presented in Fig (7) . It shows that the removal percent of Sm(III) ion increased from 57.6% to 89.02 with increasing the adsorbent mass from 0.025g to 0.4g. This increase in the removal percent of metal ion was due to increasing the adsorbent mass therefore the surface area also increased this means more active sites are available for metal ion sorption process. It was concluded that the optimum V/m =100, this percent was chosen according to its removal percent is high and the resin mass is low (0.1g) compared with V/m=25 where its removal percent is slightly high and the resin mass used (0.4g) was four times higher than the resin mass used to obtain V/m=100.

3.2 Equilibrium isotherm

$$\frac{C_e}{q_e} = \frac{1}{bQ_o} + \frac{C_e}{Q_o} \quad (6)$$

Where Q_o is the maximum adsorption capacity (mg/g), b is the Langmuir constant (L/mg) related to the energy of adsorption which reflects the affinity between the adsorbent and adsorbate.

A plot C_e/q_e versus C_e Fig (8) yields a straight line with slope 1/Q_o and intercepts 1/bQ_o. The values of Langmuir equation parameters are given in Table (3). The Langmuir model effectively and significantly described the sorption data with the R² values were 0.992, 0.989, 0.996 and 0.99 for for sorption of La³⁺, Ce³⁺, Nd³⁺ and Sm³⁺ onto POTZr(IV)WP at 25 °C respectively. According to the Q_m (mgg⁻¹) parameter, monolayer capacity at 25 °C of POTZr(IV)WP was arranged in the following sequence, Sm > La > Nd > Ce. These metals seem to reach saturation, which means that the metal had clogged possible available sites in POTZr(IV)WP and further adsorption could take place only at new surfaces [18-19]. Also, from Table (3) it is observed an increase of the saturation capacity with increase of

temperature which reflects a better accessibility of the sorption sites. Based on K_L values increase in the sequence, $Sm > La > Nd > Ce$; samarium has higher affinity for POTZr(IV)WP, which is well correlated with the higher adsorption capacity Q_m obtained.

The essential characteristics and the feasibility of the Langmuir model were expressed by [20] in terms of a dimensionless constant, commonly known as separation factor (R_L) which is expressed by the following equation:

$$R_L = \frac{1}{1 + bC_o} \quad (7)$$

The R_L values indicate either the shape of adsorption isotherm is unfavorable ($R_L > 1$) or favorable ($0 < R_L < 1$) or linear ($R_L = 1$) or irreversible ($R_L = 0$).

Values of R_L calculated at 25, 35 and 40 °C for all concentrations of studied ion solutions Table (3) were in range between 0 and 1, which indicate that the adsorption process is favorable at operation conditions studied. For each ion the R_L value decreases with the rise of temperature, suggesting an increase of the affinity between lanthanide ions and POTZr(IV)WP.

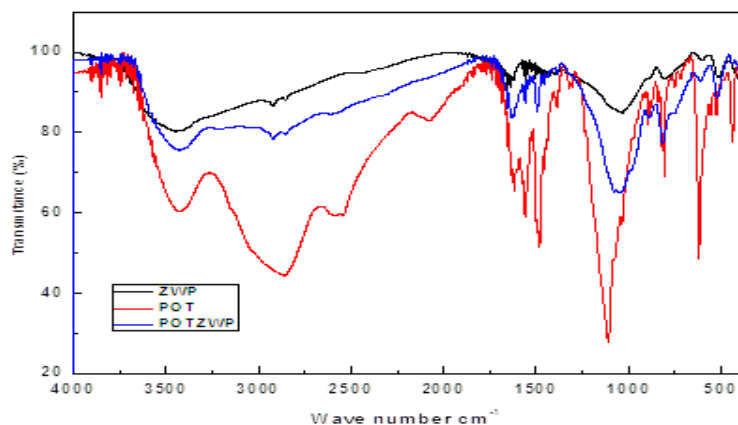


Fig (1) FTIR spectra of Zr(IV)WP, POT and POTZr(IV)WP.

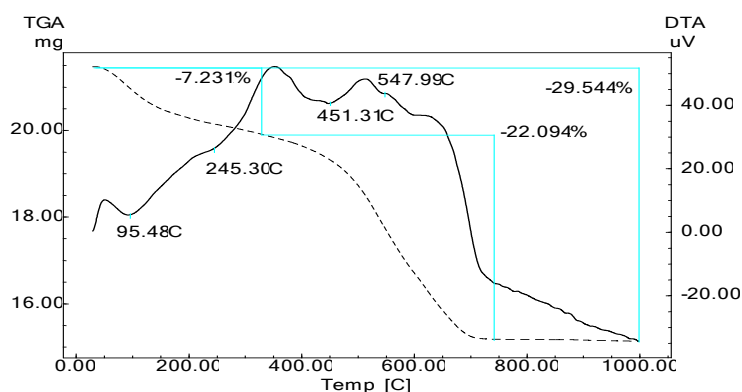


Fig (2) TGA-DTA of POTZr(IV)WP composite material.

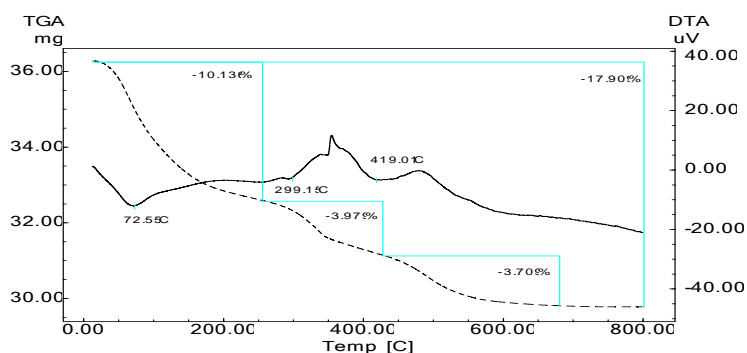
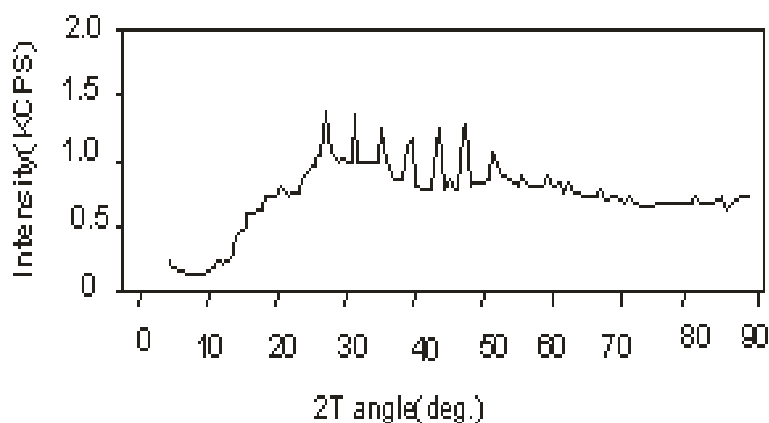


Fig (3) TGA-DTA of Zr(IV)WP inorganic adsorbent.

Table (1) Preparation conditions of various samples of POTZr(IV)WP hybrid cation exchange materials.

Samples	Mixing volume ratio (v/v)			Mixing volume ratio (v/v) of 0.05M O-toluidine	Surfactants	Appearance after drying	Na ⁺ ion exchange Capacity (meq./g)
	ZrOCl ₂ . 8H ₂ O	Na ₂ WO ₄ . 2H ₂ O	H ₃ PO ₄				
S-1	1(0.1M)	1(0.1M)	-	-	-	White granules	0.11
S-2	1(0.1M)	1(0.1M)	-	-	0.5g CTAB	White granules	0.14
S-3	1(0.1M)	1(0.1M)	-	-	0.5g SDS	White granules	0.12
S-4	1(0.1M)	1(0.1M)	-	-	1ml SDSC	White granules	0.16
S-5	1(0.1M)	1(0.1M)	-	-	0.2g CTAB (hydrothermal)	White granules	0.22
S-6	1(0.1 M)	1(0.1 M)	-	0.5	0.1g CTAB	Black shiny	0.3
S-7	2(0.1 M)	1(0.1 M)	-	0.5	0.1g CTAB	Black shiny	0.26
S-8	1(0.1 M)	2(0.1 M)	-	0.5	0.1g CTAB	Black shiny	0.38
S-9	1(0.1 M)	2(0.2 M)	-	0.5	0.1g CTAB	Black shiny	0.32
S-10	2(0.2 M)	1(0.1 M)	-	0.5	0.1g CTAB	Black shiny	0.1
S-11	1(0.2M)	2(0.1M)	-	0.5	0.1g CTAB	Black shiny	0.28
S-12	1(0.1 M)	2(0.1 M)	0.5(1M)	0.5	0.1g CTAB	Black shiny	0.44
S-13	1(0.1 M)	2(0.1 M)	0.5(4M)	0.5	0.1g CTAB	Black shiny	0.8
S-14	1(0.1 M)	2(0.1 M)	0.5(8M)	0.5	0.1g CTAB	Black shiny	0.92
S-15	1(0.1 M)	2(0.1 M)	0.5(4M)	0.5(0.1M)	0.1g CTAB	Black shiny	0.98
S-16	1(0.1 M)	2(0.1 M)	0.5(4M)	0.5(0.15M)	0.1g CTAB	Black shiny	1.32
S-17	1(0.1 M)	2(0.1 M)	0.5(4M)	0.5(0.28M)	0.1g CTAB	Black shiny	1.8
S-18	1(0.1 M)	2(0.1 M)	0.5(4M)	0.5(0.28M)	0.2g CTAB	Black shiny	1.3
S-19	1(0.1 M)	2(0.1 M)	0.5(4M)	0.5(0.28M)	0.3g CTAB	Black shiny	1.5

**Fig (4)** XRD pattern of POTZWP composite cation exchanger.**Table (2)** Chemical stability of POTZr(IV)WP in various solvents.

Solvent Concentration, M	Amount dissolved (mg/L)				
	HCl	HNO ₃	NaOH	CH ₃ COOH	H ₂ O
0.1	4.0	2.0	10.0	2.0	not detected
0.5	10.0	6.0	16.0	4.0	-
1.0	28.0	22.0	30.0	10.0	-
2.0	40.0	35.0	-	12.0	-
3.0	85.0	80.0	-	14.0	-
4.0	110.0	105.0	-	16.0	-
5.0	150.0	140.0	-	40.0	-

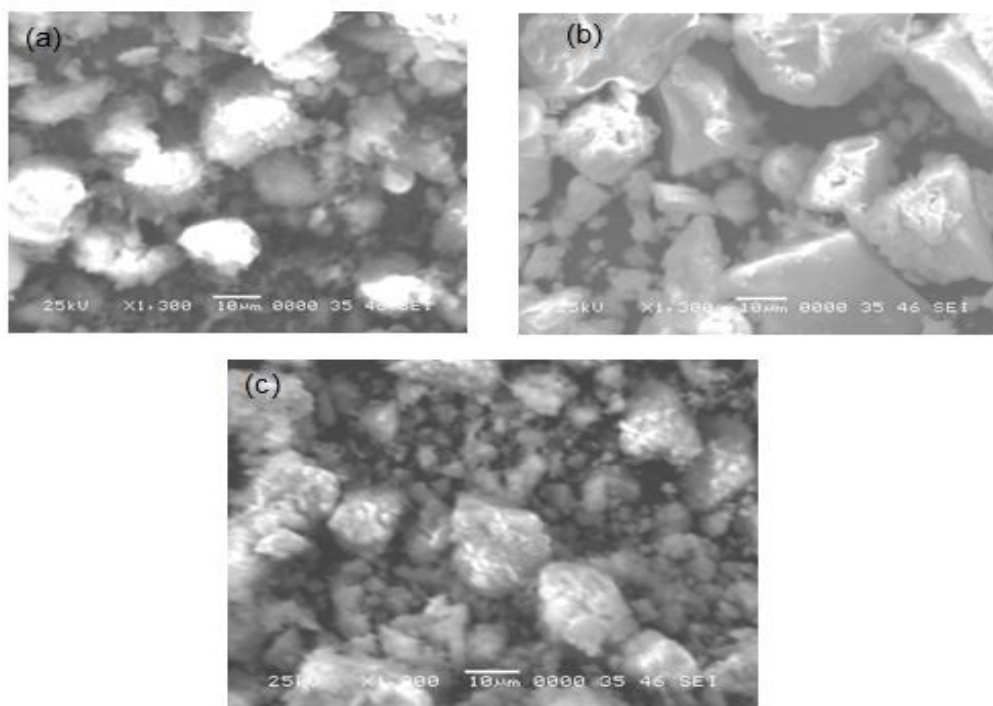


Fig (5) Scanning electron microphotograph(SEM) of (a)poly-o-toluidine(POT) , (b)Zr(IV)WP and (c)POTZr(IV)WP at magnification of 1,300

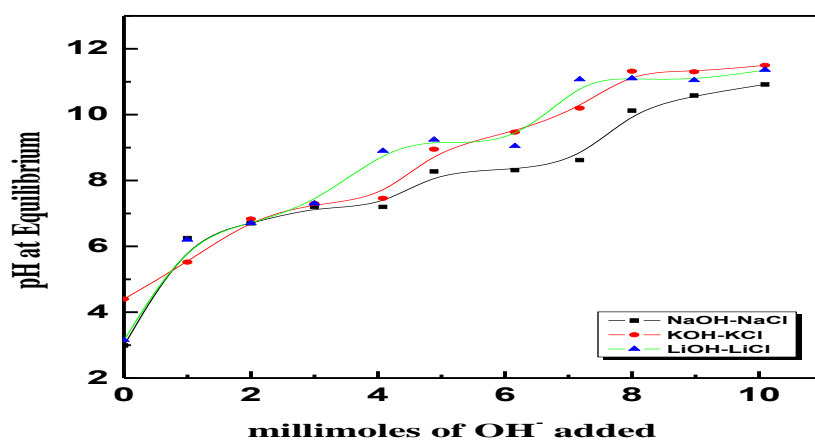


Fig (6) pH titration curve of LiCl-LiOH ,NaCl-NaOH and KCl-KOH onto POTZr(IV)WP.

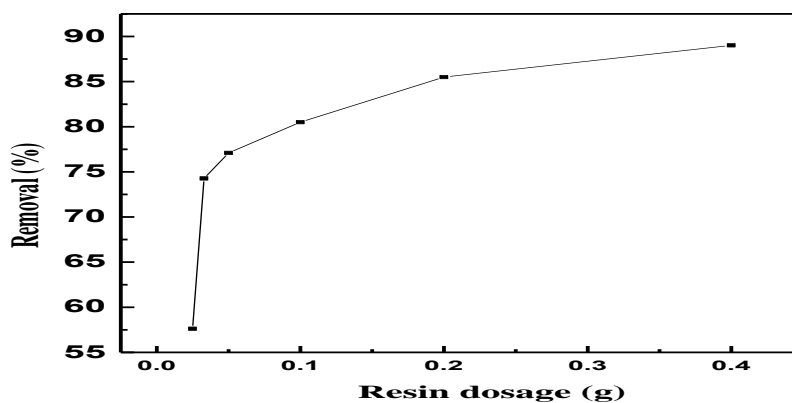


Fig (7) Effect of resin dosage on sorption of Sm(III) onto POTZr(IV)WP.

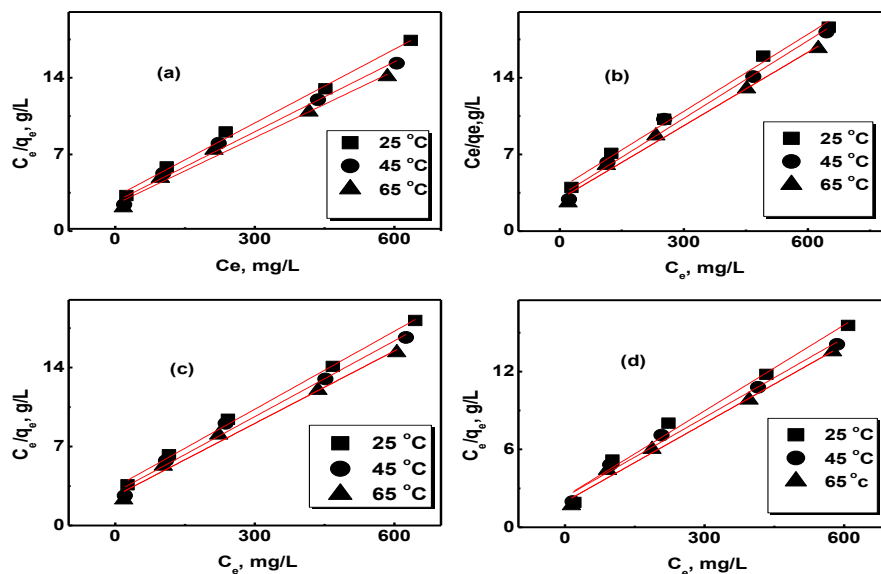


Fig (8) Langmuir isotherm model plots of La³⁺, Ce³⁺, Nd³⁺ and Sm³⁺ ion sorption onto POTZr(IV)WP at different temperatures

3.2.1 Freundlich isotherm

In 1906, Freundlich has proposed the earliest known sorption equation. It can be apply to non-ideal adsorption or multilayer sorption of adsorbate on heterogeneous surface based on the following assumptions: (1) the heat of adsorption decrease with increase of surface coverage of adsorbent; (2) the adsorption sites on the surface of adsorbent have different adsorption energies.

At present, Freundlich isotherm is widely used in different heterogeneous systems [21] and is expressed by the following equation: $\log q_e = \log K_F + \frac{1}{n} \log C_e$ (8)

Where q_e is the adsorbed amount of metal ion (mg/g), C_e is the equilibrium concentration of metal ion (mgL^{-1}), K_F represents the adsorption capacity for a unit equilibrium concentration, while $1/n$ is the indicative of the energy or intensity of the reaction and suggests the favorability and capacity of the adsorbent–adsorbate system. The values of Freundlich isotherm constants (K_F and $1/n$) determined from the linear plot of $\log q_e$ versus $\log C_e$ (Fig. 9) are presented in Table (3).

Similarly to RL values from Langmuir isotherm, the $1/n$ value indicates the type of isotherm as follows: irreversible ($1/n = 0$), favorable ($0 < 1/n < 1$), or unfavorable ($1/n > 1$). The Freundlich constants, $1/n$, shown in Table 3 indicate that La³⁺, Ce³⁺, Nd³⁺ and Sm³⁺ ions were adsorbed favorably by POTZr(IV)WP at all the different temperatures. The adsorption capacity (K_F) at 25 oC of POTZr(IV)WP was arranged in the following sequence, $\text{Sm} > \text{La} > \text{Nd} > \text{Ce}$ and is observed that its value increases with the increase of temperature. This sequence agreement with monolayer capacity Q_m that calculated from Langmuir isotherm. The R₂ values were 0.976, 0.981, 0.974 and 0.983 for sorption of La³⁺, Ce³⁺, Nd³⁺ and Sm³⁺ onto

POTZr(IV)WP at 25 oC respectively. The values of R₂ of Langmuir values are higher than Freundlich values. It can be seen that a good fitting of Langmuir model to experimental data is achieved. Similar behavior was observed in adsorption process of Cs⁺ on polyaniline titanotungstate composite cation exchanger [22].

3.2.2 Dubinin–radushkevich isotherm

Another equation used in the analysis of adsorption isotherms was proposed by Dubinin and Radushkevich [23].

The model was used to estimate the apparent free energy of adsorption as well as to make a difference between physical and chemical adsorption process. The D–R equation was given by the following relationship:

$$\ln q_e = \ln Q_m - K \varepsilon^2 \quad (9)$$

where Q_m is the theoretical saturation capacity, K is the activity coefficient related to mean sorption energy and ε is the Polanyi potential given by:

$$\varepsilon = R_g T \ln \left(1 + \frac{1}{C_e} \right) \quad (10)$$

where R is the gas constant (8.314 kJ/(mol K)) and T is the temperature (K).

The values of isotherm constants (Q_m and K) obtained by plotting $\ln q_e$ versus ε^2 (Fig. 10) are given in Table (3). The D–R constant can give the valuable information regarding the mean energy of adsorption by the following equation:

$$E = (-2K)^{-0.5} \quad (11)$$

It is known that the magnitude of E gives the information about the type of adsorption process: physical (1–8 kJ/mol), ion exchange (9–16 kJ/mol) and chemical (>16 kJ/mol) [24]. The apparent free energies of La³⁺, Ce³⁺, Nd³⁺ and Sm³⁺ adsorption on POTZr(IV)WP at the different

temperatures were calculated to be in the range of 9.26–11.47 kJ/mol, which means that the process is

ion exchange adsorption.

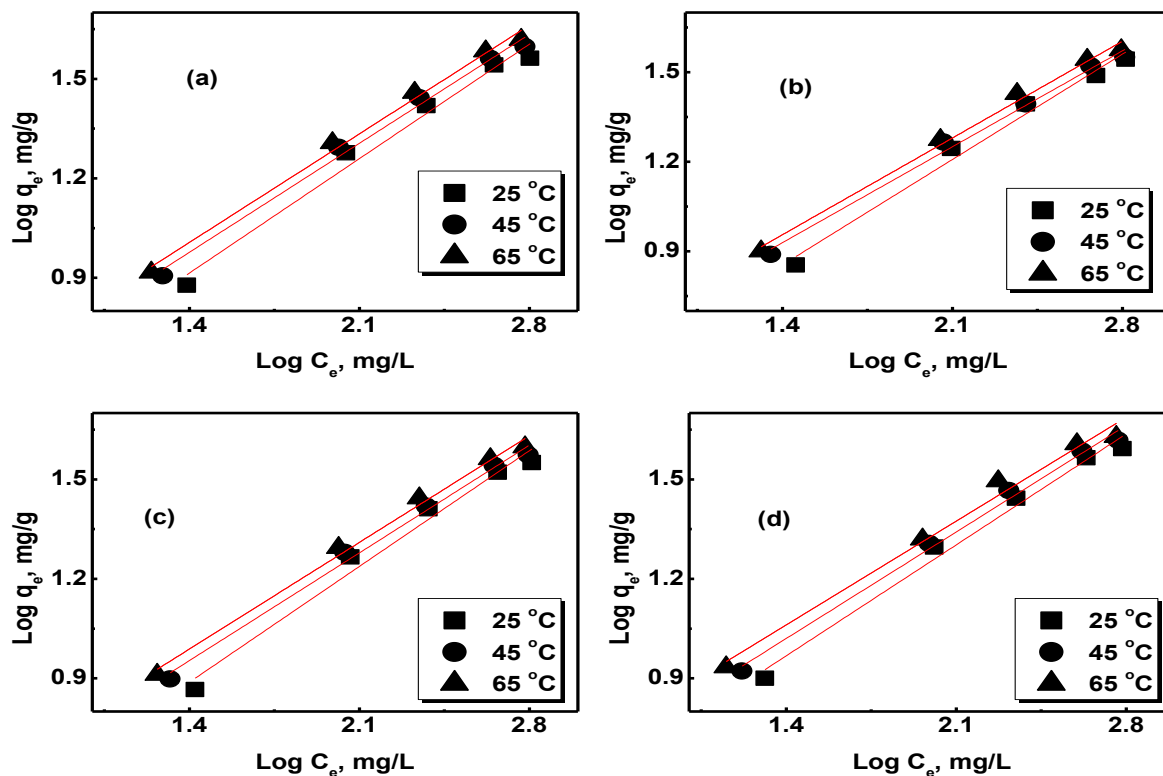


Fig (9) Freundlich isotherm model plots of La^{3+} , Ce^{3+} , Nd^{3+} and Sm^{3+} ion sorption onto POTZr(IV)WP at different temperatures.

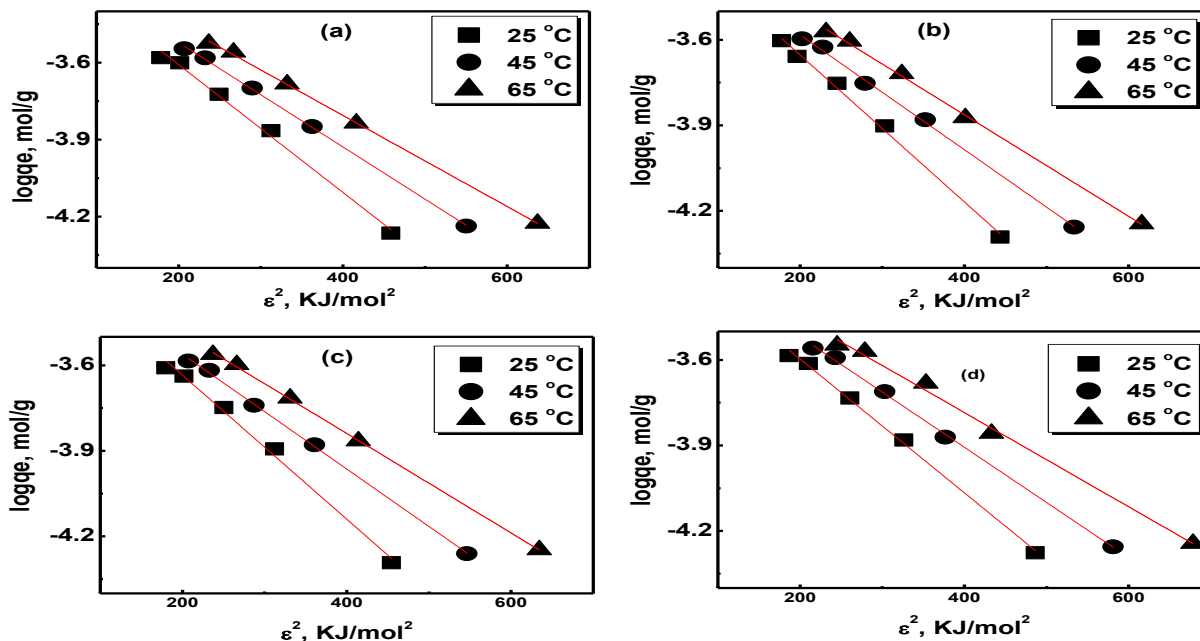


Fig (10) D-R isotherm model plots of La^{3+} , Ce^{3+} , Nd^{3+} and Sm^{3+} ion sorption onto POTZr(IV)WP at different temperature

3.2.3 Temkin isotherm

Temkin and Pyzhev isotherm was proposed to describe for the first time the adsorption of hydrogen onto platinum electrodes within the acidic solution [24-25]. The assumptions made on the Temkin adsorption model are that: (a) adsorption is

characterized by a uniform distribution of binding energies; (b) the heat of adsorption of all the molecules in the layer would decrease linearly with coverage due to adsorbent–adsorbate interactions. The linear form of Temkin isotherm was given below:

$$q_e = b \ln A + b \ln C_e \quad (12)$$

Where b is the Temkin constant related to the heat of adsorption (J/mol) and A is the equilibrium binding constant corresponding to the maximum binding energy (L/mg).

By plotting q_e against ln C_e Fig (11) it can be obtained the Temkin constants A and b as intercept and slope. The values of the Temkin parameters are given in Table 3. The Temkin constant b for the adsorption of La³⁺, Ce³⁺, Nd³⁺ and Sm³⁺ on POTZr(IV)WP was ≤ 6.91x10⁻⁵ KJmol⁻¹ at different temperatures. The low value of b confirmed that the interaction between metal ions and the POTZr(IV)WP surface was week and ion exchange was the most suggested mechanism [26]. Based on correlation coefficient shown in Table (3) the results indicate that the Langmuir and Dubinin–Radushkevich models represent a better fit of experimental data than Freundlich and Temkin models.

Thermodynamic studies

The thermodynamic parameters including Gibbs free energy (ΔG°), enthalpy (ΔH°), and entropy changes (ΔS°) can be calculated using the following equations (Smith and Van Ness, 1987) [27];

$$\Delta G^\circ = -RT \ln K_c \quad (13)$$

where R is the universal gas constant (8.314 J mol⁻¹ K⁻¹), T is the temperature (K), and K_d is the equilibrium constant. The K_d value was calculated using following equation;

$$K_c = q_e / C_e \quad (14)$$

where q_e (mg L⁻¹) and C_e (mg L⁻¹) are the equilibrium concentration of metal ions adsorbed onto POTZr(IV)WP and remained in the solution, respectively. The enthalpy (ΔH°) and entropy (ΔS°)

changes of adsorption were estimated from the following equation;

$$\Delta G^\circ = \Delta H^\circ - T \Delta S^\circ \quad (15)$$

This equation can be written as;

$$\ln K_c = \frac{\Delta S^\circ}{R} - \frac{\Delta H^\circ}{RT} \quad (16)$$

According to Eq. (16) the ΔH_o and ΔS_o were calculated from the slope and intercept of the plot between ln K_d versus 1/T, respectively as in Fig (12) and Table (4). All these relations are valid when the enthalpy change remains constant in the temperature range. The ΔG_o values were obtained by using Eq. (13) in the temperature of 25, 45 and 65 oC. The negative values of ΔG_o, for La³⁺, Ce³⁺, Nd³⁺ and Sm³⁺ ions, suggested the feasibility of the present adsorption process and spontaneous nature of the adsorption of La³⁺, Ce³⁺, Nd³⁺ and Sm³⁺ ions onto POTZr(IV)WP Table (4). On the other hand the magnitude of ΔG_o increased with increasing the temperature indicated that a better adsorption is actually obtained at higher temperatures. The positive values of ΔH_o, for these ions, indicated that the endothermic nature of adsorption process which was also supported by the increase in amount of metal uptake with the rise in temperature. One possible explanation of endothermicity of heats of adsorption is may be due to the sorption process of metal ions onto adsorbent material requires at first solvation of these ions. In order for the metal ions to be adsorbed, they have to lose part of their hydration sheath and dehydration process of ions required energy so the water removing process from ions is endothermic process [28]. The positive ΔS_o values suggested an increase in the randomness at the solid/solution interface during the adsorption of La³⁺, Ce³⁺, Nd³⁺ and Sm³⁺ onto POTZr(IV WP [24].

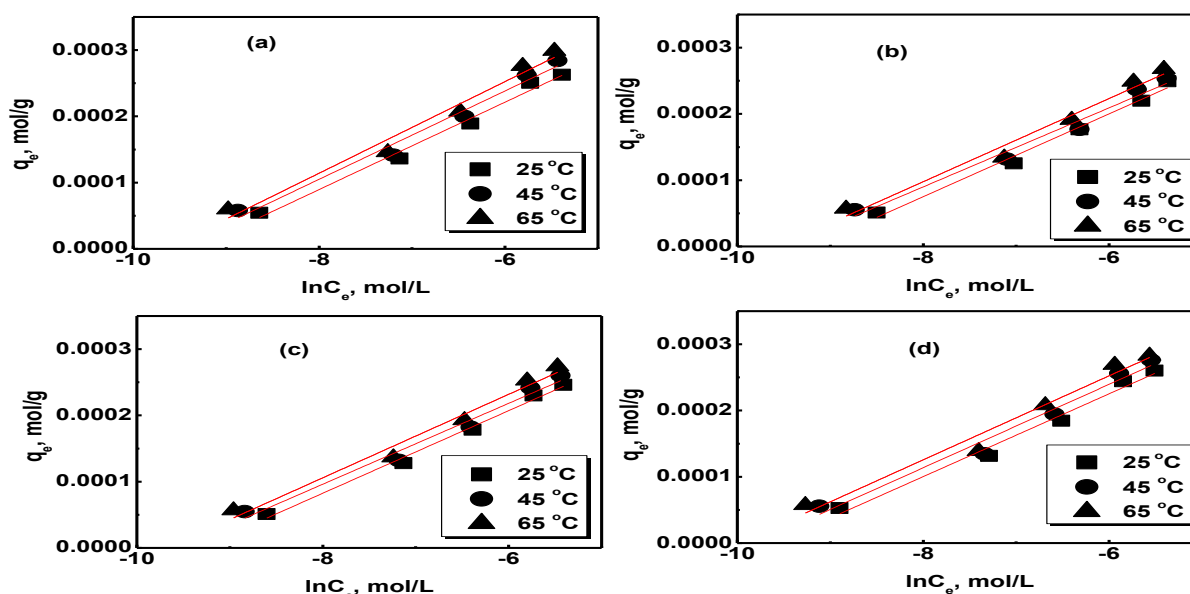


Fig (11) Temkin isotherm model plots of La³⁺, Ce³⁺, Nd³⁺ and Sm³⁺ ion sorption onto POTZr(IV)WP at different temperatures.

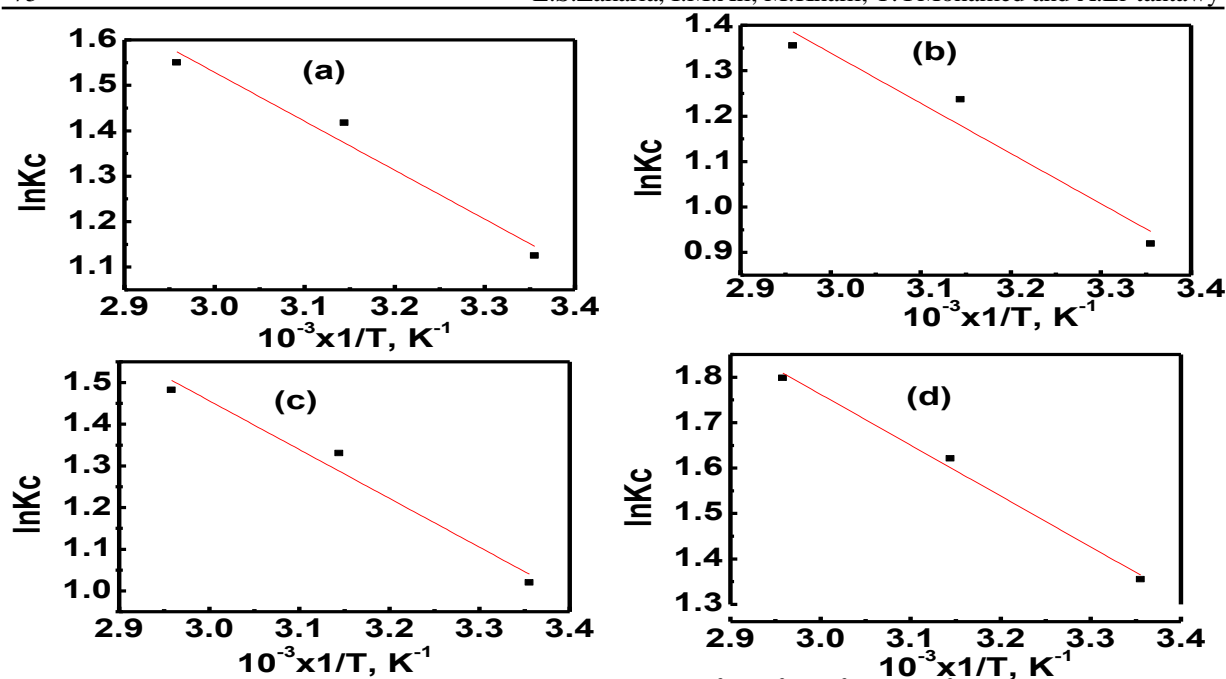


Fig (12) Plots of $\ln K_c$ versus $1/T$ for the sorption processes of La^{3+} , Ce^{3+} , Nd^{3+} and Sm^{3+} of onto POTZr(IV)WP.

Table (3) Langmuir, Freundlich, D-R and Temkin isotherm model parameters for sorption of La^{3+} , Ce^{3+} , Nd^{3+} and Sm^{3+} onto POTZr(IV)WP composite material at different reaction temperatures.

Isotherm Models	Lanthanum			Cerium			Neodymium			Samarium		
	25°C	45°C	65°C	25°C	45°C	65°C	25°C	45°C	65°C	25°C	45°C	65°C
Langmuir Parameters												
$Q_m(\text{mgg}^{-1})$	44.54	47.01	49.33	42.61	42.33	44.72	43.38	44.66	46.68	46.93	48.99	49.58
$K_L(\text{Lg}^{-1}) * 10^{-3}$	7.12	7.8	8.20	6.0	7.33	7.62	6.77	7.59	8.13	7.86	8.65	10.21
R^2	0.992	0.987	0.984	0.989	0.982	0.985	0.996	0.984	0.985	0.99	0.985	0.988
Freundlich Parameters												
$1/n$	0.493	0.469	0.468	0.504	0.459	0.463	0.498	0.464	0.459	0.477	0.458	0.447
$K_F(\text{mg}^{1-1/n})L^{1/n}(\text{g}^{-1})$	1.68	2.09	2.25	1.41	1.94	2.03	1.55	2.02	2.22	1.99	2.39	2.72
R^2	0.976	0.989	0.991	0.981	0.989	0.991	0.974	0.99	0.991	0.983	0.991	0.983
D-R Parameters												
$Q_m(\text{molg}^{-1}) * 10^{-4}$	7.77	7.68	8.02	7.28	6.61	7.07	7.22	7.42	6.94	7.45	7.38	7.53
$K(\text{mol}^2\text{KJ}^{-2}) * 10^{-3}$	5.73	4.69	4.00	5.94	4.65	4.09	4.00	5.82	4.62	4.62	4.46	3.79
R^2	0.993	0.992	0.999	0.995	0.997	0.998	0.999	0.992	0.999	0.997	0.998	0.993
$E(\text{KJmol}^{-1})$	9.33	10.31	11.04	9.17	10.36	11.04	11.17	9.26	10.39	9.61	10.57	11.47
Temkin Parameters												
$B * 10^{-5}$	6.59	6.66	6.91	6.25	5.96	6.27	6.23	6.1	6.3	6.25	6.29	6.33
$A * 10^3$	11.64	13.98	14.26	9.89	1.20	1.43	11.04	13.46	16.03	14.76	18.20	21.00
R^2	0.984	0.975	0.969	0.984	0.971	0.97	0.99	0.97	0.97	0.98	0.967	0.965

Table (5) Thermodynamic parameters of La^{3+} , Ce^{3+} , Nd^{3+} and Sm^{3+} sorbed onto POTZr(IV)WP.

Metal ion	$\Delta G^\circ(\text{KJ/mol})$			$\Delta H^\circ(\text{kJ/mol}) * 10^{-3}$	$\Delta S^\circ(\text{J/mol K})$	R^2
	25°C	45 °C	65 °C			
La^{3+}	-2.78	-3.74	-4.35	8.95	39.59	0.937
Ce^{3+}	-2.27	-3.26	-3.81	9.19	38.71	0.904
Nd^{3+}	-2.52	-3.51	-4.16	9.72	41.34	0.949
Sm^{3+}	-3.35	-4.28	-4.94	9.31	42.59	0.987

4. Conclusion

POTZr(IV)WP was successfully prepared to obtain favored ion exchange material with Na⁺ ion exchange capacity (1.8 meq./g). It was found that POTZr(IV)WP has properties differ from Zr(IV)WP and poly-o- toluidine. Sorption behavior of La³⁺, Ce³⁺, Nd³⁺ and Sm³⁺ onto POTZr(IV)WP obeyed to Langmuir isotherm model and D-R which confirmed that the most proposed mechanism was ion exchange. The mean energy of adsorption *E* determined in the D–R equation revealed that the adsorption onto natural stevensite is controlled by an ion-exchange mechanism. Thermodynamic parameters were calculated and found to be spontaneous and endothermic in nature.

References

- [1] J.V.Carolan, T.L.Hanley, V.Luca, Zirconium organophosphonates as high capacity, selective lanthanide Sorbents, Separation and Purification Technology , PP.129, 150–158, 2014.
- [2] J.Mukherjee, J.Ramkumar, S.waran, R.Shukla, A.K.Tyagi, Sorption characteristics of nano manganese oxide: efficient sorbent for removal of metal ions from aqueous streams, Journal of Radioanalytical and Nuclear Chemistry DOI 10.1007/s10967-012-2393-7.
- [3] A.Demirbas, E.Pehlivan, F.Gode, T.Altun, G.Arslan, Adsorption of Cu(II), Zn(II), Ni(II), Pb(II), and Cd(II) from aqueous solution on Amberlite IR-120 synthetic resin, Journal of Colloid and Interface Science, vol.282 , pp.20–25, 2005.
- [4] I.M.Ali, Y.H.Kotp, I.M.El-Naggar, Desalination, 259,228, 2010.
- [5] I.El-Naggar, E.Zakaria , I.Ali, Aspects of the adsorption behavior of Cu²⁺, Zn²⁺ and Ni²⁺ ions on lithium titanate ion exchanger, Separation Science and Technology, 39 (4), 2004.
- [6] A.I.Zakaria, E.I.El-Naggar, Radiotracer study on the adsorption of Cs-134 on stannic silicate ion exchanger, Arab Journal of Nuclear Science and technology, vol.37 (2), pp.31–42, 2004.
- [7] A.E.Zakaria, H.I.Aly, .Adsorption behavior of ¹³⁴Cs and ²²Na ions on tin and titanium ferrocyanides, Adsorption, pp. 10 ,45–50, 2004.
- [8] K.G.Varshney, M.Z.A.Rafiquee, Somya,A, Triton X-100 based cerium (IV) phosphate as a new Hg(II) selective,surfactant based fibrous ion exchanger: Synthesis, characterization and adsorption behavior, Colloids and Surfaces A: Physicochem. Eng. Aspects, P.317 ,400–405, 2008.
- [9] A.Khan, S. Shaheen, Synthesis and characterization of a novel hybrid nano composite cation exchangerpoly-o-toluidine Sn (IV) tungstate: Its analytical applications as ion-selectiveelectrode, Solid State Sciences, PP.16, 158-167, 2013.
- [10] M.F.Attallah, E.H.Borai, R.Harjula, A.Paajanen, M.Karesoja and R.Koivula, Journal of Materials Science and Engineering B, vol.1, p.736, 2011.
- [11] A.P.Gupta, P.K.Varshney, Reactive & Functional Polymers, pp.32,67, 1997.
- [12] N.E.Topp, K.W.Pepper, Properties of ion-exchange resins in relation to their structure. Part I. Titration curves. Journal of Chemical Society, PP.99–303, 1949.
- [13] M.M.Abd El-Latif, M.F.Elkady, Kinetics study and thermodynamic behavior for removing cesium, cobalt and nickel ions from aqueous solution using nano-zirconium vanadate ion exchanger, Desalination, PP.271, 41–54, 2011.
- [14] I.Ali, Journal of Radioanalytical and Nuclear Chemistry, vol.260(1), p.149-157, 2003.
- [15] I.M.Ali, E.S.Zakaria, M.M.Ibrahim, I.M.El-Naggar, Synthesis, structure, dehydration transformations and ion exchange characteristics of iron-silicate with various Si and Fe contents as mixed oxides, Polyhedron, PP.27, 429–439,2008.
- [16] A.A.Khan, Inamuddin, Preparation, physico - chemical characterization, analytical applications and electrical conductivityof cation-exchanger: PolyanilineSn (IV) phosphate, Reactive , Functional Polymers , PP.66,1649–1663, 2006.
- [17] N.S.A.Akhtar, A.Khan, Md.D.A, M.A.Khan, Synthesis, characterization and electrical conductivity of Polyaniline-Sn (IV) tungstophosphate hybrid cation exchanger: Analytical application for removal of heavy metal ions from wastewater, Desalination, PP.340, 73–83, 2014.
- [18] S.Vasilu, I.Bunia, S.Racovita, V.Neagu, Adsorption of cefotaxime sodium salt on polymer coated ion exchange resin microparticles: Kinetics, equilibrium and thermodynamic studies, Carbohydrate Polymers, PP.85, 376–387, 2011.
- [19] H.S.Ibrahim, T.S.Jamil, E.Z.Hegazy, Application of zeolite prepared from Egyptian kaolin for the removal of heavy metals: II. Isotherm models, Journal of Hazardous Materials, vol.182, 842–847, 2010.
- [20] T.W.Weber, R.K.Chakravot, Pore and solid diffusion models for fixed bed adsorbents. AiChE Journal, vol.20, pp.228–238, 1974.
- [21] M.Monier, D.M.Ayad, Y.Weil, A.A.Sarhan, Adsorption of Cu(II), Co(II) and Ni(II) ions by modified magnetite chitosan chelating resinmeasurement studies of an ‘organic–inorganic’ composite, Journal of Hazardous Materials, PP.177, 962–970, 2010.

- [22] M.Khalil,, Chemical studies on poly aniline titanotungstate as anew composite cation exchanger and its analytical applications for removal of cesium from aqueous solution, PhD thesis, Ain shams university, 2012.
- [23] M.M.Dubinin, E.D.Zaverina, L.I.V. Radushkevich, Sorption and structure of active carbons Adsorption of organic vapors. Zhurnal Fizicheskoi Khimii, 21, 1351–1362, 1947.
- [24] M.Chabani, A.Amrane, A.Bensmaili., Kinetic modelling of the adsorption of nitrates by ion exchange resin. Chemical Engineering Journal, 125, 111–117, 2006.
- [25] M.I.Temkin, V.Pyzhev, Kinetics of ammonia synthesis on promoted iron catalyst. Acta Physico Chemica USSR, PP.12, 327–356, 1940.
- [26] R.R.Sheha, E.Metwally, Equilibrium isotherm modeling of cesium adsorption onto magnetic materials, Journal of Hazardous Materials, vol.143, pp.354-361, 2007.
- [27] J.M.Smith, H.C.Van Ness, Introduction to Chemical Engineering Thermodynamics, fourth ed. McGraw-Hill, Singapore, 1987.
- [28] I.Mobasherpour, E.Salahi, M.pazouki, Removal of nickel(II) from aqueous solutions by using nano-crystalline calcium hydroxyapatite, Journal of Saudi Chemical Society, vol.15, pp.105-112, 2011.